Influence of resonance charge exchange on the resolution and contrast of a field-ion image

P. A. Bereznyak and I. M. Mikhaĭlovskiĭ

Physico-technical Institute, Ukrainian Academy of Sciences
(Submitted February 7, 1973)
Zh. Eksp. Teor. Fiz. **65**, 475–480 (August 1973)

The variation of the resolution and contrast of a field-ion image with increase of pressure of the filling gas is investigated. A characteristic asymmetry of the blurring of the image points and the appearance of duplicate points of comparatively low intensity is observed. It is demonstrated quantitatively that charge-exchange processes are predominant among the various types of interactions between the field ions and the filling gas.

The field-ion microscopy is the only method which provides an experimental means for the direct observation of the atomic structure of the object being investigated. The range of its applications is wide: from fundamental problems in the physics of crystals with defects[1] to various metal-physics applications.[2-4] However, many basic problems in the method itself have not yet been resolved. For example, the essence of the mechanism responsible for the strong deterioration of the quality of field-ion images on increase of the filling gas pressure from 10^{-3} to 10^{-2} Torr has not yet been established. The fall of the resolution and contrast of a field-ion image of the surface of a micro-crystal on increase of the pressure of the imaging gas is usually attributed to the elastic scattering of the field-emitted ions through small angles on interaction with the gas molecules.[5] The scattering is regarded as attraction to a dipole induced by the electric field of the ion. However, we shall show that the deterioration in the resolution and contrast with increasing gas pressure is accompanied by effects which cannot be explained by the elastic scattering of ions.

Our experiments were carried out in a helium field-emission microscope with liquid-nitrogen cooling of the sample. The helium pressure was varied within the range 5×10^{-4}–2×10^{-2} Torr. It was usually difficult to observe changes in the dimensions and shape of the field images of the surface atoms because of the superposition of the images of individual atoms. The number of atoms contributing to a field-ion image was reduced by forming hemispherical microprojections of $50-100$ Å in diameter on an initially atomically smooth surface. This was done by the use of a decelerated vacuum arc.[6] The microprojections were then evaporated by a field of $400-450$ MV/cm and this process was stimulated by a nitrogen pressure of 8×10^{-6}–10^{-5} Torr. The preferential evporation of the peripheral regions of the projections enabled us to form ring- and disk-shaped projections.[7] The microrelief of these projections was stabilized by reducing the partial pressure of nitrogen to $\sim 10^{-7}$ Torr.

The image of the surface of a sample treated as described above is shown in Fig. 1a. The helium pressure p_{He} was 2×10^{-3} Torr; the distance between the top of a projection and the screen was 80 mm. Broadening of the image was observed when p_{He} was increased to 5×10^{-3} Torr. Figure 1b shows a field-ion photomicrograph of the same sample for $p_{He} = 10^{-2}$ Torr. A comparison of the photomicrographs in Figs. 1a and 1b demonstrates that the broadening of the field-ion pattern on increase in the pressure was accompanied by the elongation of the images of individual atoms toward the periphery. It is worth noting that the size of the "streaks" which appeared was approximately propor-
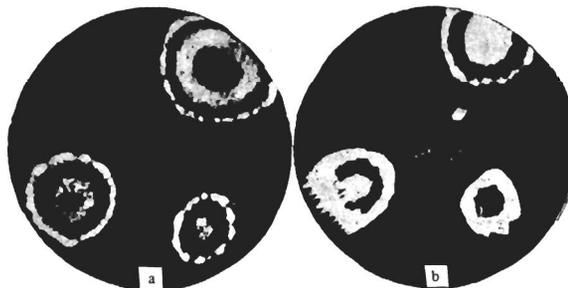

FIG. 1. Field-ion images of ring-shaped microprojections on the surface of a tungsten sample, obtained at two helium pressures: a–2×10^{-3} Torr; b–10^{-2} Torr.

tional to the distance from the stereographic center of the field-ion pattern and that the resolution decreased accordingly (Fig. 1b).

It is also clear from Fig. 1b that an increase in the gas pressure gave rise to relatively weak duplicate images of all three microprojections. The magnification of these duplicate images was several times smaller than the magnification of the main images; the duplicates were located between the main images and the stereographic center. In field-ion photomicrographs of samples with hemispherical dips, the duplicate images of individual atoms merged and produced a diffuse background in the central part of the pattern, which reduced the contrast and resolution in this region.

The pressure at which these effects appeared depended strongly on the electrode configuration. Thus, when screening electrodes were used in order to increase the brightness of the image of small-radius points,[8,9] the broadening of the central part of the pattern by the duplicate images was observed at pressures as low as $(2-4) \times 10^{-3}$ Torr and the threshold pressure decreased with increasing screening coefficient. By way of example, Figs. 2a and 2b show two field-ion images for samples of approximately the same geometry: one of these images (a) was obtained without the use of a screening electrode; the other (b) was recorded employing an electrode which ensured that the screening coefficient was 4. In both cases, the helium pressure was 4×10^{-3} Torr. The distance between the tip and the luminescent screen was 100 mm. A strong diffuse background was observed in the central {110} part of a screened point (Fig. 2b).

These effects, which accompany an increase in the pressure of the imaging gas, cannot be explained on the basis of the generally accepted model.[5] However, they can be understood if we allow for symmetric charge exchange, whose importance has already been pointed out for microscopes with specially constructed electrodes.[1] Under charge exchange conditions a fast
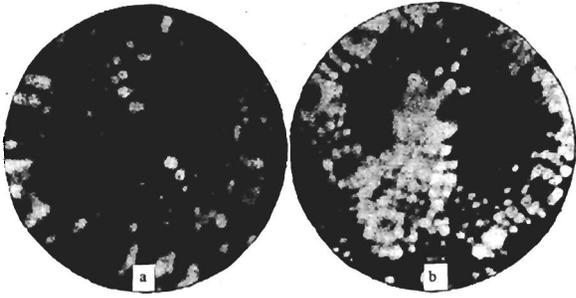
FIG. 2. Field-ion images of unscreened (a) and screened (b) tungsten emitters; $p_{He} = 4 \times 10^{-3}$ Torr.

"primary" ion is scattered through a very small angle and having been converted to a neutral atom it travels further linearly without interacting with the electric field. Depending on the part of the trajectory at which charge exchange takes place, the point at which such an atom reaches the screen will lie further from or closer to the point at which we would expect the original ion to reach the luminescence screen. Thus, an image point is converted into a "streak" directed toward the perimeter of the screen. The images of the atoms located on the periphery of the pattern are deformed to a greater degree because the trajectories of the ions which would reach this region in the absence of charge exchange are bent more than in the axial region. The calculations given below show that the greater proportion of the charge exchange events occurs far from the tip in regions where the electric field gradient is weak. Therefore, the slow "secondary" ions form an almost parallel beam because they are unable to acquire much energy in their transit to the screen. These ions are responsible for the weak diffuse background in the central part of a field-ion image.

The proposed explanation can be checked quantitatively if know the trajectories of the ions that have not suffered charge exchange and the trajectories of the charge exchange products as a function of the point where such charge exchange occurs. The equations of motion of a charged particle in the field of a point electrode are obtained in[10]. For a positive ion these equations are

$$\ddot{\gamma} = \omega\gamma(\gamma^2 + \eta^2)^{-1/2} + \gamma(\gamma^2 + \eta^2)^{-1/4}[(\gamma^2 + \eta^2)^{1/4} + \eta]^{-1},$$

$$\ddot{\eta} = \omega\eta(\gamma^2 + \eta^2)^{-1/2} + (\gamma^2 + \eta^2)^{-1/4};$$

(1)

where γ and η are the dimensionless cylindrical coordinates of the ion,

$$\gamma = \rho/r_0, \quad \eta = z/r_0 \qquad (2)$$

(r_0 is the radius of the point at its tip), and ω is a parameter which varies with the shape of the tip and is assumed in our calculations to be 4. The time in Eq. (1) is measured in units of

$$\tau = r_0\left[\frac{M}{eV}\left(\omega - \frac{\omega}{\eta_{max}} + \ln\eta_{max}\right)\right]^{1/2}. \qquad (3)$$

Here, e and M are the charge and mass of an ion; V is the potential difference between the tip and the screen; η_{max} is the dimensionless distance between them. For He^+ ions, $r_0 = 0.4\,\mu$, $V = 10^4$ V, and 8 cm from the screen ($\eta_{max} = 2 \times 10^5$), we find that $\tau = 3.3 \times 10^{-12}$ sec.

The solution of the system (1) on a computer yielded the trajectories and velocities of the primary helium ions and of the ions formed as a result of charge exchange. The system (1) was integrated by the Runge-

Kutta method in which the error in the determination of the coordinates, velocities, and energies of particles did not exceed 0.5%. By way of example, Fig. 3 gives the trajectory of a primary ion emerging from the tip of a point at an angle of 45° with respect to the symmetry axis, as well as the trajectories of neutral products of charge exchange (He atoms) and of secondary ions formed during charge exchange.

The symmetric charge exchange (He^+, He) cross section has been determined for a wide range of energies with a high precision[11,12] and the knowledge of the law of motion of an He^+ ion makes it possible to calculate the probability of charge exchange as a function of the position of this ion l on its trajectory. Between the point $l = 4r_0$ and the screen, the cross section σ decreases from 7.8×10^{-16} to 5.8×10^{-16} cm^2. Therefore, we shall use the average value

$$\bar{\sigma} = \frac{1}{L}\int_0^L \sigma(l)\,dl = 5.94 \cdot 10^{-16}\ [\text{cm}^2];$$

here, L is the total length of the trajectory.

In order to obtain the distribution of the brightness in the main and duplicate images on the screen, we must allow for the dependence of the brightness Φ of the luminescence of the screen on the energy of the incident particle. In the case of ionoluminescence, as in the case of the luminescence resulting from the impact of neutral atoms, this dependence is of the form[13,14]

$$\Phi \propto (E - E_0)^\alpha, \qquad (4)$$

where the "dead" potential E_0 and the power exponent α vary strongly with the type of phospher and the nature of the ion or atom. We used a standard zinc sulfide coating (FS-4) and assumed that, in the case of ionoluminescence in helium, $E_0 = 1.5$ keV and $\alpha = 1$.

Since the probability of a transit of a primary ion to the screen without charge exchange is $\exp(-n\bar{\sigma}L)$ and the initial density of the ion flux along the trajectory is proportional to the number of atoms n of the imaging gas per unit volume, i.e., to the pressure of this gas p, the brightness Φ of an image point can be represented by

$$\Phi \propto (V - E_0)p\exp\{-n\bar{\sigma}L\}. \qquad (5)$$

In calculating the distribution of the brightness in a streak associated with a main image point, we shall divide this streak into segments of length $\Delta\gamma$. The brightness of the luminescence emitted by each such segment is

$$\Delta\Phi \propto n^2 \int_{(\Delta l)} [E(l) - E_0]\bar{\sigma}\exp\{-n\bar{\sigma}l\}\,dl, \qquad (6)$$

where the integral is calculated over that part of the trajectory of the primary ion from which the charge exchange products reach the region $\Delta\gamma$ of the screen. The energy $E(l)$ of a neutral atom formed as a result of charge exchange is equal to the energy $E_1(l)$ of the primary ion at the charge exchange point and it remains constant right up to the screen. Performing the integration (6) over different parts of the screen, we obtain the distribution of the brightness in a streak near an image point.

In comparing the brightness in Eqs. (5) and (6) we must bear in mind that the minimum diameter of an image point, set by the quantum-mechanical and thermal broadening, is about 0.5 mm. The total distri-

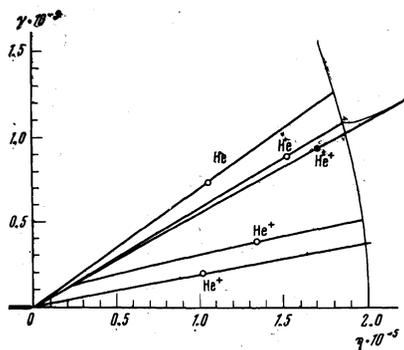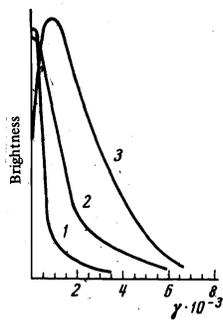P. A. Bereznyak and I. M. Mikhailovskii

FIG. 3

FIG. 4

FIG. 3. Trajectories of a primary ion (identified by a black dot) and of products of its charge exchange (open circles) in the chamber of a field-ion microscope. The distributions of the brightness in the main and duplicate images on the screen are shown schematically on the right.

FIG. 4. Distribtuions of the brightness in the main image obtained for different pressures of the filling gas: $1-5 \times 10^{-3}$ Torr; $2-10^{-2}$; $3-2 \times 10^{-2}$ Torr. The origin of the coordinates is assumed to be located at the point of incidence of the primary ions which have not suffered charge exchange.

bution of the brightness in a spot image of an atom on the screen is shown in Fig. 4 for different pressures. A segment of a streak can be regarded as invisible if its brightness is below that of a main image point obtained for $p_{He} = 10^{-4}$ Torr. It is clear from Fig. 4 that the broadening due to the charge exchange becomes significant at pressures of 5×10^{-3} Torr; at 10^{-2} Torr the streaks are about 1.5 mm long ($r_0 = 4 \times 10^{-5}$ cm) and at 2×10^{-2} Torr the brightness maximum begins to shift in accordance with the dependence $\Phi(p)$ given by Eq. (5) and its maximum occurs at $5 \times 10^{-3}-10^{-2}$ Torr; outside this range the brightness falls rapidly.

The brightness of a duplicate image can be calculated in the same way, using Eq. (6), but $E(l)$ now represents the energy of a secondary ion resulting from charge exchange at the point l, the energy of this ion being measured at the moment of its impact on the screen:

$$E(l) = V - E_1(l),$$

and the value of Δl is found by analyzing the trajectories of real secondary ions.

Such calculations show that the visible luminescence can be generated only by secondary ions formed in a small segment of the trajectory from $l = 100r_0$ to $l = 800r_0$. They all reach the same point on the screen

and the scatter is $\sim 500r_0$, i.e., about 0.2 mm. Therefore, a sharp duplicate image of an atom, separated by a considerable distance from the main image, is obtained (Fig. 3). However, the brightness of this image at $p_{He} = 2 \times 10^{-2}$ Torr is almost 20 times less than the brightness of the main image and at lower pressures it should not be observed at all. It should be pointed out that the brightness of a duplicate image is very sensitive to the value of E_0 and, therefore, the contrast may be improved by the use of a phosphor with a higher E_0.

The authors are grateful to V. V. Slezov for discussing the results.

[1] E. W. Müller and T. T. Tsong, Field Ion Microscopy: An Introduction to Principles, Experiments, and Applications, American Elsevier, New York, 1969.

[2] B. Ralph, Surface Sci. 23, 130 (1970).

[3] R. I. Garber, B. G. Lazarev, L. S. Lazareva, I. M. Mikhaĭlovskiĭ, and N. N. Sidorenko, Zh. Eksp. Teor. Fiz. 63, 1359 (1972) [Sov. Phys.-JETP 36, 718 (1973)].

[4] I. M. Mĭkhailovskiĭ and Zh. I. Dranova, Zh. Eksp. Teor. Fiz. 63, 567 (1972) [Sov. Phys.-JETP 36, 300 (1973)].

[5] E. W. Müller, Advan. Electron. Electron Phys. 13, 83 (1960).

[6] A. P. Komar, V. P. Savchenko, and V. N. Shrednik, Dokl. Akad. Nauk SSSR 129, 540 (1959) [Sov. Phys.-Dokl. 4, 1286 (1960)].

[7] I. M. Mikhaĭlovskiĭ and N. N. Sidorenko, Fiz. Tverd. Tela, 13, 824 (1971) [Sov. Phys.-Solid State 13, 680 (1971)].

[8] E. W. Müller and O. Nishikawa, Rev. Sci. Instrum., 36, 556 (1965).

[9] R. I. Garber, Zh. I. Dranova, I. M. Mikhaĭlovskiĭ, and G. G. Chechel'nitskiĭ, Prib. Tekh. Eksp. No. 1, 204 (1969).

[10] P. A. Bereznyak and V. V. Slezov, Radiotekh. Ekektron. 17, 354 (1972).

[11] S. W. Nagy, W. J. Savola, Jr., and E. Pollack, Phys. Rev. 177, 71 (1969).

[12] W. N. Shelton and P. A. Stoycheff, Phys. Rev. A, 3, 613 (1971).

[13] C. F. Eve and H. E. Duckworth, Can. J. Phys. 36, 104 (1958).

[14] B. M. Nosenko and N. A. Strukov, Izv. Akad. Nauk SSSR, Ser. Fiz. 25, 314 (1961).